*Electronic supplementary information*

# Electronic and geometric effects in an Au@NiO core-shell nanocatalyst on the oxidative esterification of aldehydes

Shaoqi Zhan,*[1] Haohong Song[2],Zili Wu,[3,4] and De-en Jiang*[5]

[1] Department of Chemistry-Ångström, Uppsala University, Box 523, 751 20 Uppsala, Sweden

[2]Interdisciplinary Materials Science, Vanderbilt University, Nashville, Tennessee, 37235, United States

[3] Chemical Sciences Division, Oak Ridge National Laboratory, Oak Ridge, Tennessee 37831, United States

[4] Center for Nanophase Materials Sciences, Oak Ridge National Laboratory, Oak Ridge, Tennessee 37831, United States

[5] Department of Chemical and Biomolecular Engineering, Vanderbilt University, Nashville, Tennessee 37235, United States


Email: shaoqi.zhan@kemi.uu.se; de-en.jiang@vanderbilt.edu
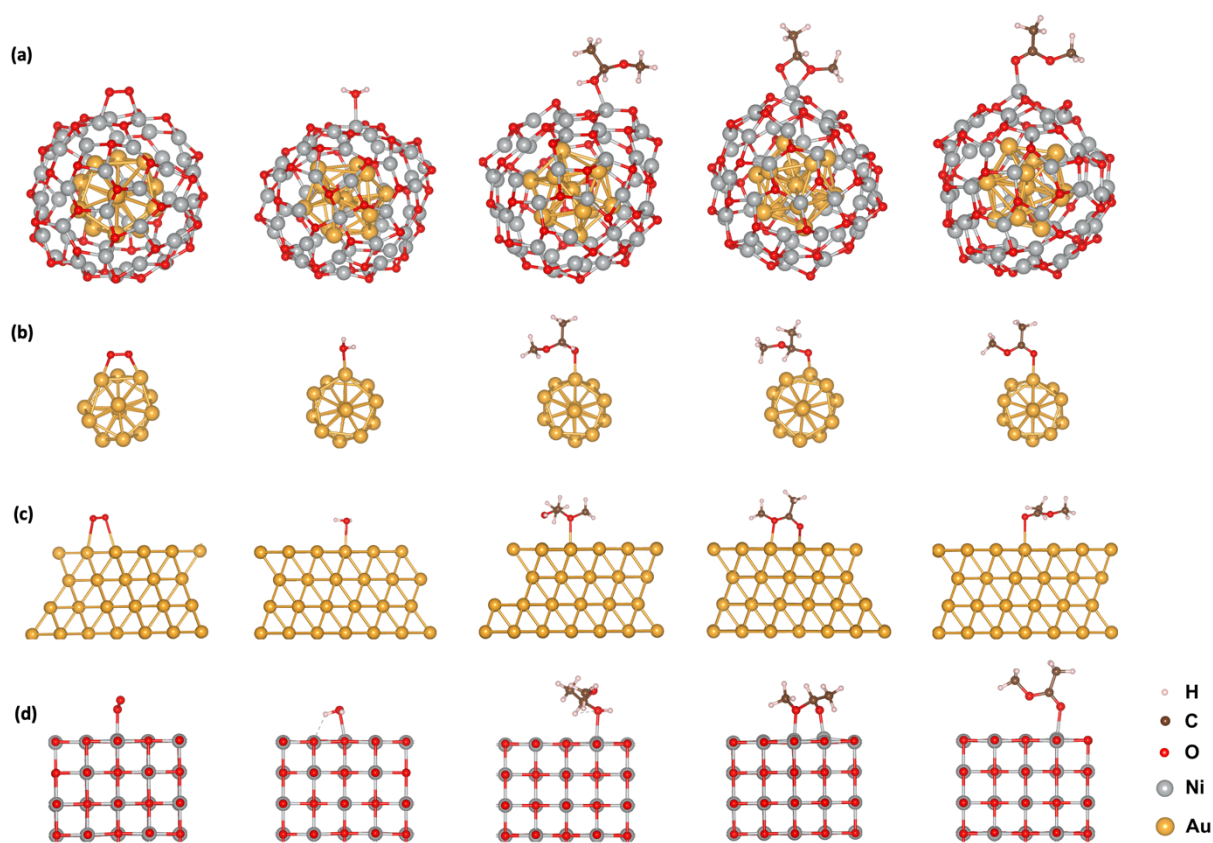
**Figure S1.** Optimized structures of $O_2$, $H_2O$, hemiacetal, deprotonated hemiacetal, and ester molecules adsorbed on the different surfaces: (a) the $Au_{13}@(NiO)_{48}$ core-shell NP; (b) $Au_{13}$; (c) $Au(111)$; (d) $NiO(100)$.
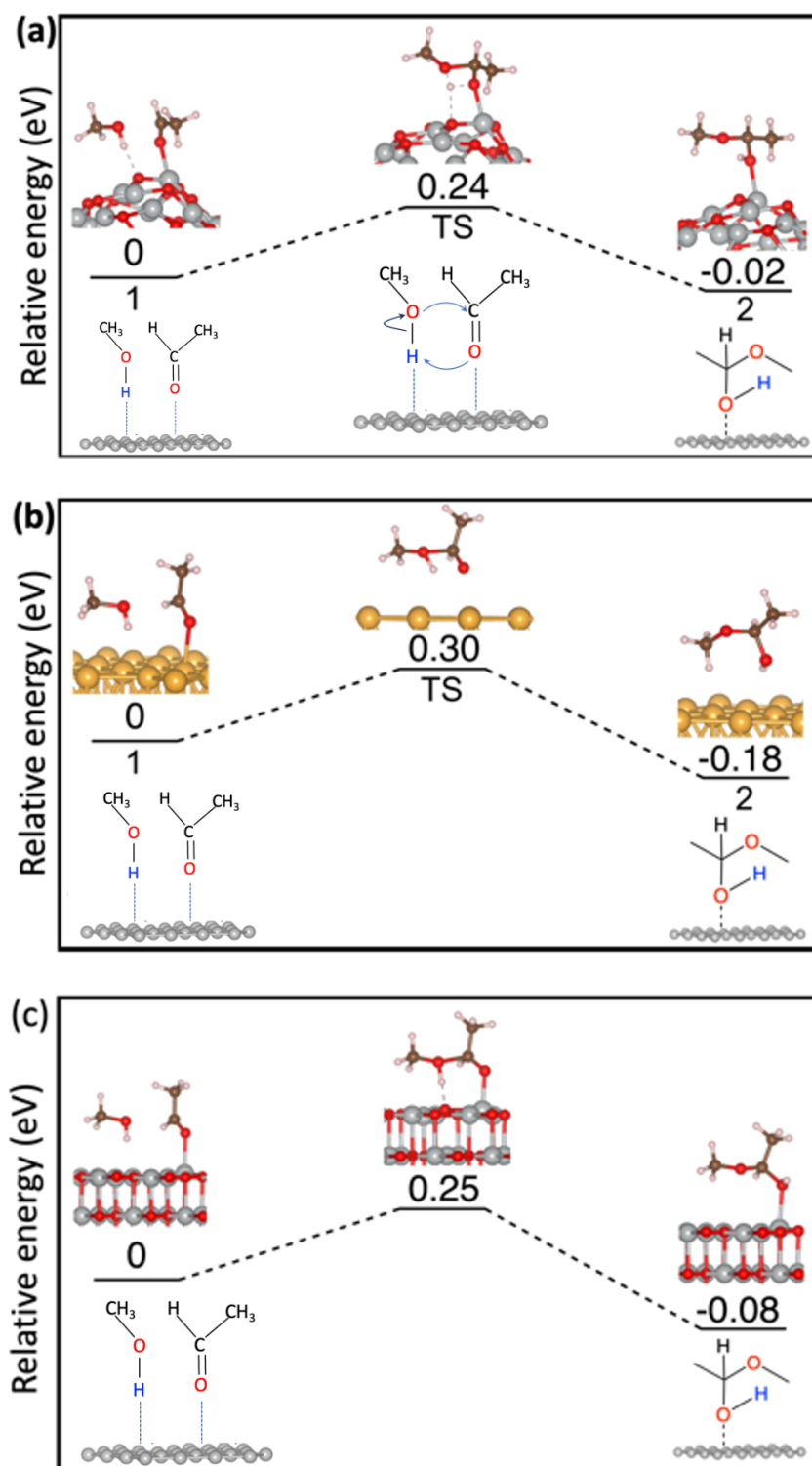
**Figure S2.** Energy profiles of the hemiacetal formation reaction: (a) on $Au_{13}@(NiO)_{48}$; (b) on $Au(111)$; (c) on $NiO(100)$. The structures exclusively display the region where molecules are adsorbed.
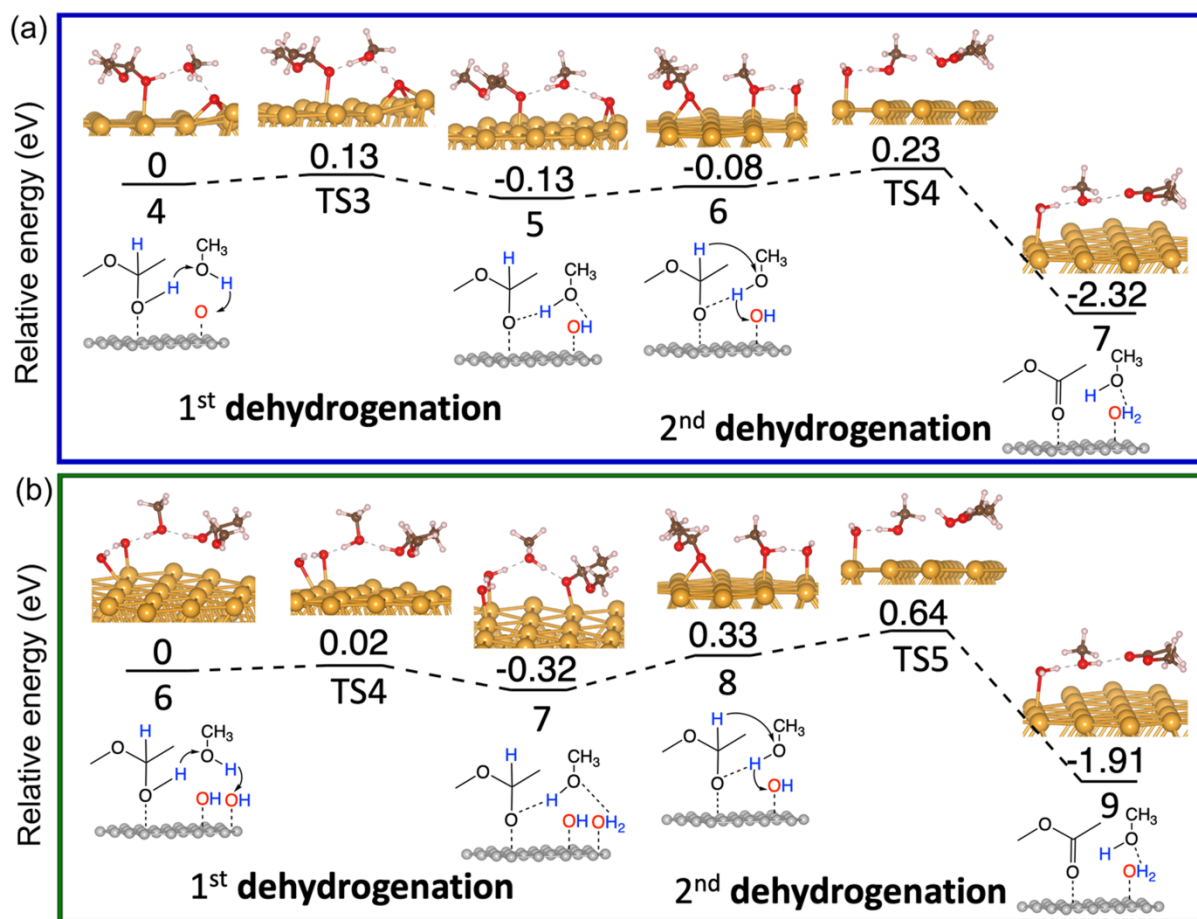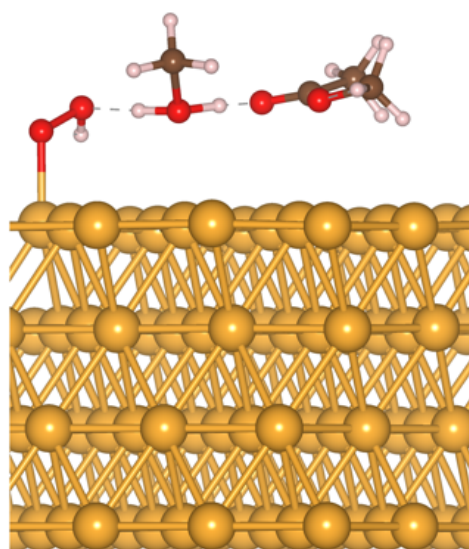
**Figure S3.** Energy profiles of oxidative dehydrogenation of the 2nd hemiacetal on Au(111): (a) via the oxo pathway; (b) via the hydrogen peroxide pathway.
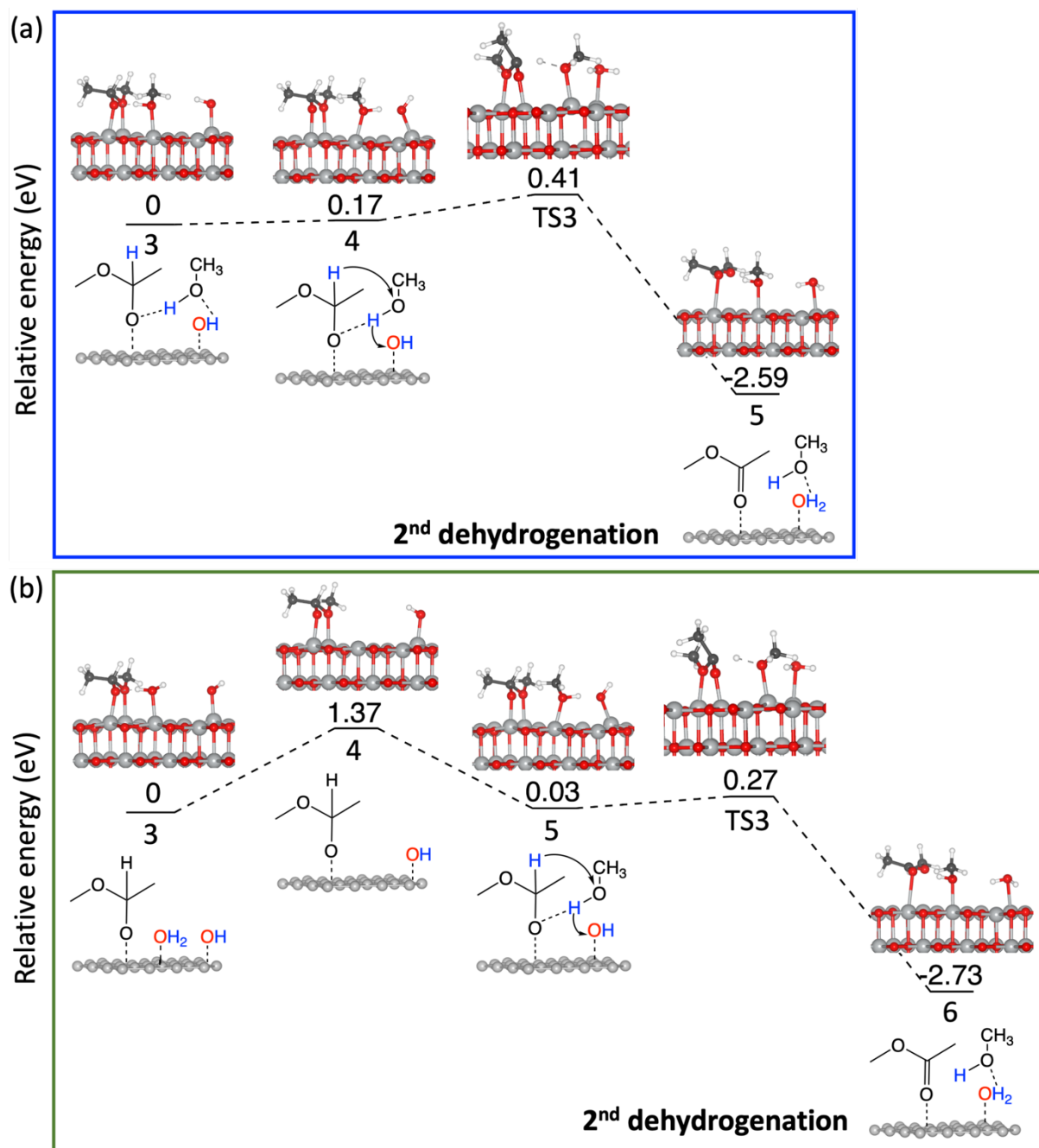
**Figure S4.** Energy profiles of oxidative dehydrogenation of the $2^{nd}$ hemiacetal on NiO(100): (a) via the oxo pathway; (b) via the hydrogen peroxide pathway.
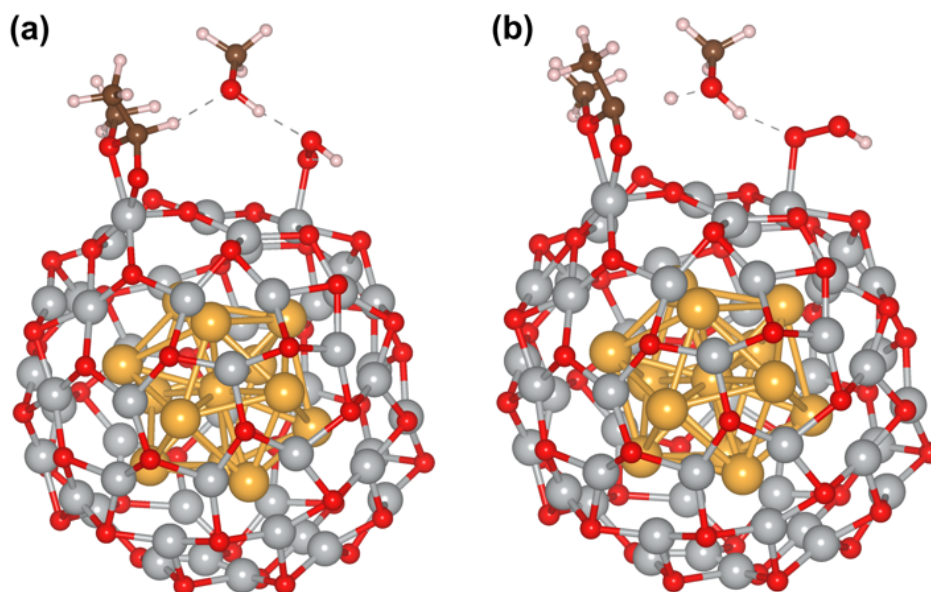
**Figure S5.** Optimized transition state structures for the dehydrogenation of the adsorbed deprotonated hemiacetal: (a) via the oxo pathway; (b) via the hydrogen peroxide pathway.



**Figure S6.** Optimized transition state of dehydrogenation of the adsorbed deprotonated hemiacetal via the oxo pathway on Au(111).
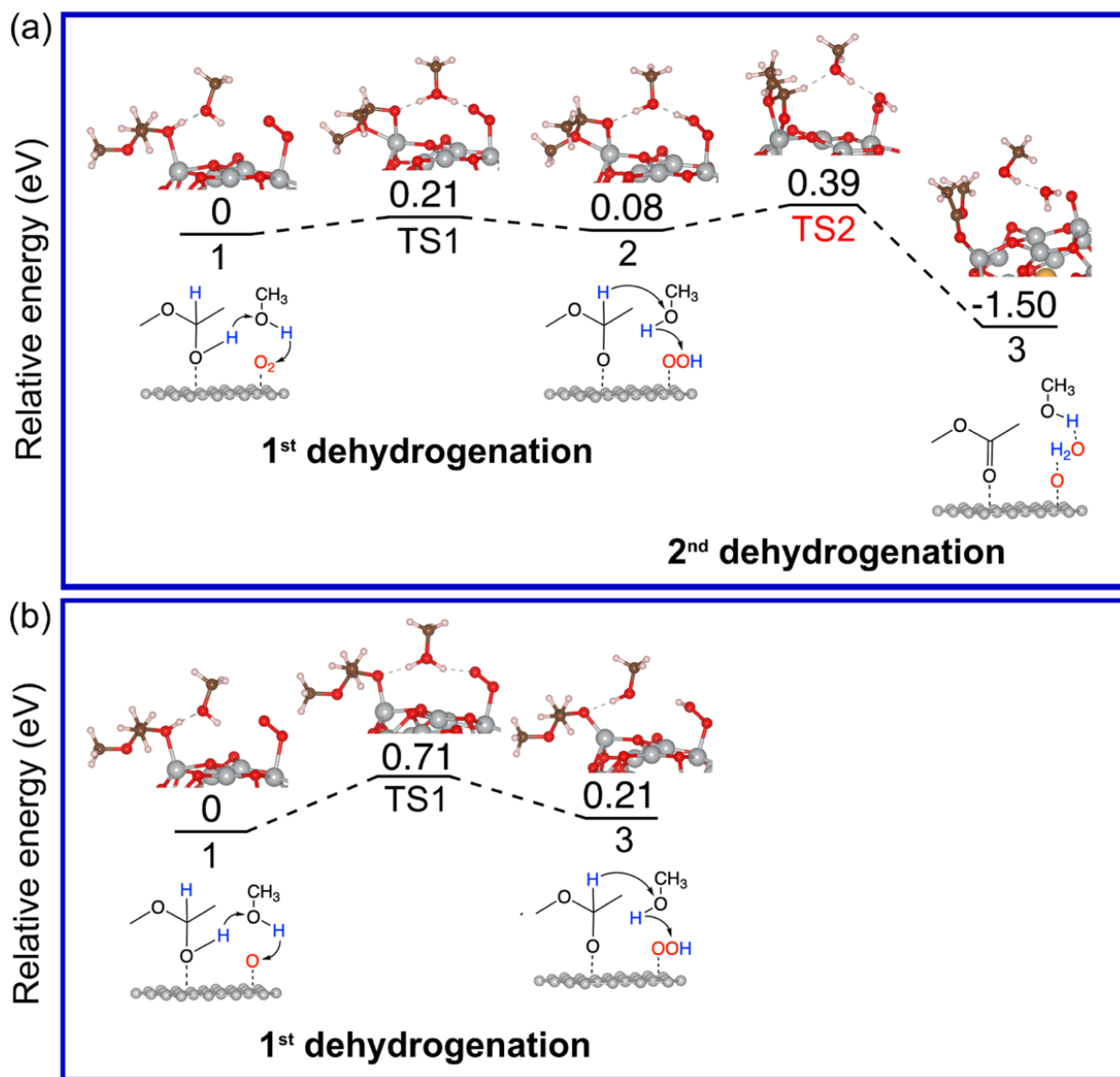
**Figure S7.** Energy profiles of the first oxidative dehydrogenation of hemiacetal $Au_{13}@(NiO)_{48}$: (a) via the bidentate adsorption mode; (b) via the monodentate adsorption mode.

**Table S1.** Adsorption energies (in eV) of four key species on $Au_{13}@(NiO)_{48}$, $Au_{13}$, Au(111), and NiO(100).

| | $Au_{13}@(NiO)_{48}$ | $Au_{13}$ | Au(111) | NiO(100) |
|---|---|---|---|---|
| **O₂** | -0.85 | -1.79 | -1.23 | -1.04 |
| **H₂O** | -0.39 | -0.44 | -0.29 | -0.66 |
| **Hemiacetal** | -0.91 | -0.66 | -0.69 | -0.84 |
| **Deprotonated hemiacetal** | -2.20 | -2.18 | -1.78 | -1.81 |
| **Ester** | -0.67 | -0.76 | -0.68 | -0.47 |

**Table S2.** Adsorption mode and energy ($E_{ad}$) of deprotonated hemiacetal on $Au_{13}@(NiO)_{48}$, Au(111), and NiO(100).

| | $Au_{13}@(NiO)_{48}$ | $Au_{13}@(NiO)_{48}$ | Au(111) | NiO(100) |
|---|---|---|---|---|
| **Mode** | Bidentate | Monodentate | Bridging | Bridging |
| **$E_{ad}$ (eV)** | -2.20 | -1.68 | -1.78 | -1.81 |

**Microkinetic modeling details**

For surface reactions, the pre-exponential factor is assumed to be $10^{11}$ s$^{-1}$, as proposed by Pal and coworkers.[1]

Adsorption processes are treated as nonactivated with the rate constant and rate per site expressed as $k_{a\,ds} = \dfrac{P \cdot A}{\sqrt{2\pi m k_B T}}$ and $r_{\text{ads}} = Pk_{\text{ads}}(1 - \theta)$, respectively.[2]

Desorption rate constant ($k_{\text{des}}$)[2] is described as $k_{des} = \dfrac{k_B T^3}{h^3} \cdot A \cdot \left(\dfrac{2\pi m k_B}{\sigma \theta rot}\right) \cdot exp\left(-\dfrac{E\,des}{RT}\right)$.

      P - the gas pressure

      A - the site surface area, approximated to be $1 \times 10^{-19}$ m$^2$

      $k_B$ - the Boltzmann constant

      T – temperature

      m - mass of reactant

      h - the Planck's constant

      $\theta$ - the coverage rate

      $\sigma$ - the sticking coefficient which has a default value of 1 for all reactions

      I - a molecular moment of inertia; see Table S4

      $\theta_{\text{rot}}$ - the rotational temperature in K ($\theta_{\text{rot}} = \dfrac{h^2}{8\pi^2 k_B I}$); see Table S4

**Table S3**. The elementary reaction steps and corresponding forward and reverse barriers used for microkinetic modelling.

| Surface_ Pathway | Elementary reaction | Forward $E_{act}$ (eV) | Backward $E_{act}$ (eV) |
|---|---|---|---|
| Au(111) _H2O2 | $CH_3OH + * \rightleftharpoons CH_3OH*$ | - | 0.69 |
| | $CH_3CH(OH)OCH_3) + * \rightleftharpoons CH_3CH(OH)OCH_3*$ | - | 0.69 |
| | $O_2 + * \rightleftharpoons O_2*$ | - | 1.23 |
| | $CH_3CH(OH)OCH_3* + O_2* + CH_3OH* \rightleftharpoons CH_3CHOOCH_3* + OOH* + CH_3OH*$ | 0.23 | 0.07 |
| | $CH_3CHOOCH_3* + OOH* + CH_3OH* \rightleftharpoons CH_3COOCH_3* + CH_3OH* + HOOH*$ | 0.81 | 2.67 |
| | $HOOH* + * \rightleftharpoons 2OH*$ | 0.37 | 1.19 |
| | $CH_3CH(OH)OCH_3* + OH* + CH_3OH* \rightleftharpoons CH_3CHOOCH_3* + H_2O* + CH_3OH*$ | 0.02 | 0.34 |
| | $H_2O + * \rightleftharpoons H_2O*$ | - | 0.29 |
| | $CH_3CHOOCH_3* + CH_3OH* + OH* \rightleftharpoons CH_3COOCH_3* + H_2O* + CH_3OH*$ | 0.31 | 2.55 |
| | $CH_3COOCH_3 + * \rightleftharpoons CH_3COOCH_3*$ | - | 0.68 |
| Au(111) _oxo | $CH_3OH + * \rightleftharpoons CH_3OH*$ | - | 0.69 |
| | $CH_3CH(OH)OCH_3 + * \rightleftharpoons CH_3CH(OH)OCH_3*$ | - | 0.69 |
| | $O_2 + * \rightleftharpoons O_2*$ | - | 1.23 |
| | $CH_3CH(OH)OCH_3* + O_2* + CH_3OH* \rightleftharpoons CH_3CHOOCH_3* + OOH* + CH_3OH*$ | 0.23 | 0.07 |
| | $CH_3CHOOCH_3* + OOH* + CH_3OH* + * \rightleftharpoons CH_3COOCH_3* + CH_3OH* + O* + H_2O*$ | 0.68 | 3.63 |
| | $CH_3CH(OH)OCH_3* + O* + CH_3OH* \rightleftharpoons CH_3CHOOCH_3* + OH* + CH_3OH*$ | 0.13 | 0.26 |
| | $H_2O + * \rightleftharpoons H_2O*$ | - | 0.29 |
| | $CH_3CHOOCH_3* + CH_3OH* + OH* \rightleftharpoons CH_3COOCH_3* + H_2O* + CH_3OH*$ | 0.31 | 2.55 |
| | $CH_3COOCH_3 + * \rightleftharpoons CH_3COOCH_3*$ | - | 0.68 |
| NiO(100) _H2O2 | $CH_3OH + * \rightleftharpoons CH_3OH*$ | - | 1.69 |
| | $CH_3CH(OH)OCH_3 + * \rightleftharpoons CH_3CH(OH)OCH_3*$ | - | 0.84 |
| | $O_2 + * \rightleftharpoons O_2*$ | - | 1.04 |
| | $CH_3CH(OH)OCH_3* + O_2* + CH_3OH* \rightleftharpoons CH_3CHOOCH_3* + OOH* + CH_3OH*$ | 0.47 | 0.20 |
| | $CH_3CHOOCH_3* + OOH* + CH_3OH* \rightleftharpoons CH_3COOCH_3* + CH_3OH* + HOOH*$ | 1.62 | 3.28 |
| | $HOOH* + * \rightleftharpoons 2OH*$ | 0.48 | 0.40 |
| | $CH_3CH(OH)OCH_3* + OH* + CH_3OH* \rightleftharpoons CH_3CHOOCH_3* + H_2O* + CH_3OH*$ | 0.10 | 0.17 |
| | $H_2O + * \rightleftharpoons H_2O*$ | - | 0.66 |
| | $CH_3CHOOCH_3* + CH_3OH* + OH* \rightleftharpoons CH_3COOCH_3* + H_2O* + CH_3OH*$ | 0.24 | 3.00 |
| | $CH_3COOCH_3 + * \rightleftharpoons CH_3COOCH_3*$ | - | 0.47 |
| NiO(100) _oxo | $CH_3OH + * \rightleftharpoons CH_3OH*$ | - | 1.69 |
| | $CH_3CH(OH)OCH_3 + * \rightleftharpoons CH_3CH(OH)OCH_3*$ | - | 0.84 |
| | $O_2 + * \rightleftharpoons O_2*$ | - | 1.04 |
| | $CH_3CH(OH)OCH_3* + O_2* + CH_3OH* \rightleftharpoons CH_3CHOOCH_3* + OOH* + CH_3OH*$ | 0.47 | 0.20 |
| | $CH_3CHOOCH_3* + OOH* + CH_3OH* + * \rightleftharpoons CH_3COOCH_3* + CH_3OH* + O* + H_2O*$ | 1.63 | 3.20 |
| | $CH_3CH(OH)OCH_3* + O* + CH_3OH* \rightleftharpoons CH_3CHOOCH_3* + OH* + CH_3OH*$ | 0.17 | 0.26 |
| | $H_2O + * \rightleftharpoons H_2O*$ | - | 0.66 |
| | $CH_3CHOOCH_3* + CH_3OH* + OH* \rightleftharpoons CH_3COOCH_3* + H_2O* + CH_3OH*$ | 0.41 | 3.00 |
| | $CH_3COOCH_3 + * \rightleftharpoons CH_3COOCH_3*$ | - | 0.47 |
| Au@NiO _H2O2 | $CH_3OH + * \rightleftharpoons CH_3OH*$ | - | 0.64 |
| | $CH_3CH(OH)OCH_3 + * \rightleftharpoons CH_3CH(OH)OCH_3*$ | - | 0.91 |
| | $O_2 + * \rightleftharpoons O_2*$ | - | 0.85 |
| | $CH_3CH(OH)OCH_3* + O_2* + CH_3OH* \rightleftharpoons CH_3CHOOCH_3* + OOH* + CH_3OH*$ | 0.21 | 0.13 |
| | $CH_3CHOOCH_3* + OOH* + CH_3OH* \rightleftharpoons CH_3COOCH_3* + CH_3OH* + HOOH*$ | 0.47 | 2.04 |
| | $HOOH* + * \rightleftharpoons 2OH*$ | 0.05 | 0.99 |
| | $CH_3CH(OH)OCH_3* + OH* + CH_3OH* \rightleftharpoons CH_3CHOOCH_3* + H_2O* + CH_3OH*$ | 0.10 | 0.17 |
| | $H_2O + * \rightleftharpoons H_2O*$ | - | 0.39 |
| | $CH_3CHOOCH_3* + CH_3OH* + OH* \rightleftharpoons CH_3COOCH_3* + H_2O* + CH_3OH*$ | 0.03 | 2.48 |
| | $CH_3COOCH_3 + * \rightleftharpoons CH_3COOCH_3*$ | - | 0.67 |
| Au@NiO _oxo | $CH_3OH + * \rightleftharpoons CH_3OH*$ | - | 0.64 |
| | $CH_3CH(OH)OCH_3 + * \rightleftharpoons CH_3CH(OH)OCH_3*$ | - | 0.91 |
| | $O_2 + * \rightleftharpoons O_2*$ | - | 0.85 |
| | $CH_3CH(OH)OCH_3* + O_2* + CH_3OH* \rightleftharpoons CH_3CHOOCH_3* + OOH* + CH_3OH*$ | 0.21 | 0.13 |
| | $CH_3CHOOCH_3* + OOH* + CH_3OH* + * \rightleftharpoons CH_3COOCH_3* + CH_3OH* + O* + H_2O*$ | 0.31 | 1.89 |
| | $CH_3CH(OH)OCH_3* + O* + CH_3OH* \rightleftharpoons CH_3CHOOCH_3* + OH* + CH_3OH*$ | 0.03 | 2.30 |
| | $H_2O + * \rightleftharpoons H_2O*$ | - | 0.39 |
| | $CH_3CHOOCH_3* + CH_3OH* + OH* \rightleftharpoons CH_3COOCH_3* + H_2O* + CH_3OH*$ | 0.08 | 1.56 |
| | $CH_3COOCH_3 + * \rightleftharpoons CH_3COOCH_3*$ | - | 0.67 |

**Table S4**. The rotational temperature and molecular moment of inertia used for microkinetic modelling.

| Molecular | I ($10^{-46}$kg*m$^2$) | $\theta_{rot}$(K) |
|---|---|---|
| $H_2O$ | 0.10 | 39.38 |
| $CH_3OH$ | 1.02 | 3.95 |
| $O_2$ | 1.94 | 2.08 |
| $CH_3CH(OH)OCH_3$ | 9.59 | 0.42 |
| $CH_3COOCH_3$ | 9.04 | 0.45 |

References

(1) Pal, N.; Srivastava, A.; Agrawal, S.; Rai, J. S. P. Kinetics and Mechanism of Esterification of Monoepoxies. *Materials and Manufacturing Processes* **2005**, *20* (2), 317-327.
(2) Filot, I. A. W. Introduction to microkinetic modeling. **2018,** Technische Universiteit Eindhoven.